J Comput Aided Mol Des (2014) 28:327–345
DOI 10.1007/s10822-014-9723-5

# Blind prediction of HIV integrase binding from the SAMPL4 challenge

**David L. Mobley · Shuai Liu · Nathan M. Lim · Karisa L. Wymer · Alexander L. Perryman · Stefano Forli · Nanjie Deng · Justin Su · Kim Branson · Arthur J. Olson**

Received: 27 January 2014 / Accepted: 28 January 2014 / Published online: 5 March 2014


**Abstract** Here, we give an overview of the protein-ligand binding portion of the Statistical Assessment of Modeling of Proteins and Ligands 4 (SAMPL4) challenge, which focused on predicting binding of HIV integrase inhibitors in the catalytic core domain. The challenge encompassed three components—a small "virtual screening" challenge, a binding mode prediction component, and a small affinity prediction component. Here, we give summary results and statistics concerning the performance of all submissions at each of these challenges. Virtual screening was particularly challenging here in part because, in contrast to more typical virtual screening test sets, the inactive compounds were tested because they were thought to be likely binders, so only the very top predictions performed significantly better than random. Pose prediction was also quite challenging, in part because inhibitors in the set bind to three different sites, so even identifying the correct binding site was challenging. Still, the best methods managed low root mean squared deviation predictions in many cases. Here, we give an overview of results, highlight some features of methods which worked particularly well, and refer the interested reader to papers in this issue which describe specific submissions for additional details.

**Keywords** HIV integrase · Binding mode · Virtual screening · Pose prediction · Affinity · SAMPL4

## Introduction

Accurate protein-ligand binding predictions could impact many areas of science. An ideal computational method which could quickly and reliably predict binding free energies and bound structures for small molecules of interest to arbitrary receptors would have far reaching applications, including in virtual screening, drug lead optimization, and even further afield, to help enzyme design, systems biology, and in a variety of other applications. However, most systematic tests of methods for predicting binding strengths and binding modes indicate that these still need substantial improvement to be of routine use in discovery applications. While methods can be improved based on existing

**Electronic supplementary material** The online version of this article (doi:10.1007/s10822-014-9723-5) contains supplementary material, which is available to authorized users.

D. L. Mobley (✉) · S. Liu · N. M. Lim · K. L. Wymer · J. Su
Department of Pharmaceutical Sciences and Department of Chemistry, University of California, Irvine, 147 Bison Modular, Irvine, CA 92697, USA
e-mail: dmobley@mobleylab.org

D. L. Mobley
Department of Chemistry, University of New Orleans, 2000 Lakeshore Drive, New Orleans, LA 70148, USA

A. L. Perryman · S. Forli · A. J. Olson
Department of Integrative Structural and Computational Biology, The Scripps Research Institute, La Jolla, CA 92037, USA

*Present Address:*
A. L. Perryman
Department of Medicine, Division of Infectious Diseases, Rutgers University-NJ Medical School, Newark, NJ, USA

N. Deng
Department of Chemistry and Chemical Biology Rutgers, The State University of New Jersey, A203, 610 Taylor Road, Piscataway, NJ 08854, USA

K. Branson
Hessian Informatics, LLC. 609 Lakeview Way, Emerald Hills, CA, USA

experimental data, methodological improvements need to be tested in a predictive setting to determine how well they work prospectively, and especially so for methods involving empirical parameters which are tuned to fit previously known values. Thus, we need recurring prediction challenges to help test and advance computational methods. The Statistical Assessment of Modeling of Proteins and Ligands (SAMPL) challenge we discuss here provides one such test.

## SAMPL protein-ligand binding background

The SAMPL challenge focuses on testing computational methods for predicting thermodynamic properties of small drug-like or fragment-like molecules, including solvation free energies, host-guest binding affinities, and protein-ligand binding. The challenge started informally in 2007 at one of OpenEye Software's Customers, Users, and Programmers (CUP) meetings [40], and then was formalized as the SAMPL challenge beginning in 2008. Here, we discuss the results of the protein-ligand binding component of SAMPL4, the 4th iteration of the SAMPL challenge, which took place in 2013.

Protein-ligand binding has not been a feature of every SAMPL challenge, featuring previously only in SAMPL1 and SAMPL3. SAMPL1 included a pose prediction test on kinases, which proved extremely challenging. The system which proved most interesting for analysis was JNK3 kinase, where the best performing predictions were from two participants who used software-assisted visual modeling to generate and select poses. Essentially, pose predictions were generated and filtered using expert knowledge of related ligands or related systems. The two experts applying this strategy substantially outperformed all pure algorithmic approaches [47]. Affinity prediction results in some cases were reasonable, however [49]. The SAMPL3 protein-ligand challenge involved predicting binding of a series of fragments to trypsin [39], and a number of groups participated [2, 30, 31, 49, 50], in some cases achieving rather good enrichment for screening [49, 50] and good correlations between predicted binding strength and measured affinity [50], though the test was still challenging [31].

The current SAMPL4 challenge focused on predicting binding of a series of ligands to multiple binding sites in HIV integrase.

## HIV integrase background

According to the World Health Organizations data (http://UNAIDS.org), over 33.3 million people are currently living with an HIV infection. Approximately 2.3–2.8 million people become infected with HIV annually, and 1.7 million people die from HIV-related causes each year. Throughout the AIDS epidemic, over 32 million people have died of HIV-related causes, which makes HIV the deadliest virus plaguing humanity.

### *HIV integrase and the drugs that target it*

HIV integrase (IN) is one of three virally encoded enzymes. It performs two distinct catalytic functions called "3' processing" (which cleaves two nucleotides off of the end of the viral cDNA in a sequence-specific manner to generate reactive $CA_{OH}$–3′ termini) and the "strand transfer reaction" (which covalently attaches, or integrates, the cleaved viral cDNA into human genomic DNA, in a non-sequence-specific manner). Two drugs that target the active site of IN have been approved by the FDA for the treatment of HIV/AIDS: Raltegravir was approved in 2007, and Elvitegravir was approved in 2012 [46]. These two drugs are called INSTIs (for Integrase Strand Transfer Inhibitors). A third INSTI, Dolutegravir, is currently in late-phase clinical trials [46].

HIV integrase is an enzyme that is part of a large family of recombinases that all contain the "DDE" motif (or D,D-35-E motif) within the active site. The two Asps and one Glu are used to chelate two magnesium ions, using monodentate interactions between each carboxylate group and a magnesium [44]. This active site region is where the 3′ processing and strand transfer reactions occur. One monomer of HIV IN contains three different domains: the N-terminal domain (NTD), catalytic core domain (CCD), and the C-terminal domain (CTD) (Fig. 1). When performing catalysis (or when bound to DNA immediately before catalysis occurs), IN is a tetramer (i.e., a dimer of three-domain dimers). The NTD is an HH-CC zinc-binding domain (for the His,His-Cys,Cys motif that chelates the Zn). The CTD displays the SH3 fold and binds DNA non-specifically (to likely help position, or scaffold, the DNA and direct it towards a CCD). The CCD displays the RnaseH fold, and two monomers of the CCD form a spherical dimer. The CCD dimer contains two active site regions (i.e., one active site per monomer), which is where the advanced INSTIs all bind (i.e., they bind to the complex of the CCD with DNA). But in the full 3-domain tetramer of HIV IN bound to both viral cDNA and human genomic DNA, it is likely that only one active site per CCD dimer is involved in catalysis (due to geometric constraints). All of the crystal structures of HIV IN used in this challenge contained dimers of only the CCD. Although there are many crystal structures of HIV IN, the only structures available in the PDB contain only one or 2 domains of the full 3 domain monomer of IN, and none of the HIV IN crystal structures include any DNA. However, a similar recombinase from Prototype Foamy Virus, called PFV integrase, was recently crystallized in many different complexes by Peter Cherepanov et al. These PFV IN crystal structures often contain DNA and one of the three aforementioned advanced INSTIs (see Fig. 1) [19, 20, 21, 34, 36].

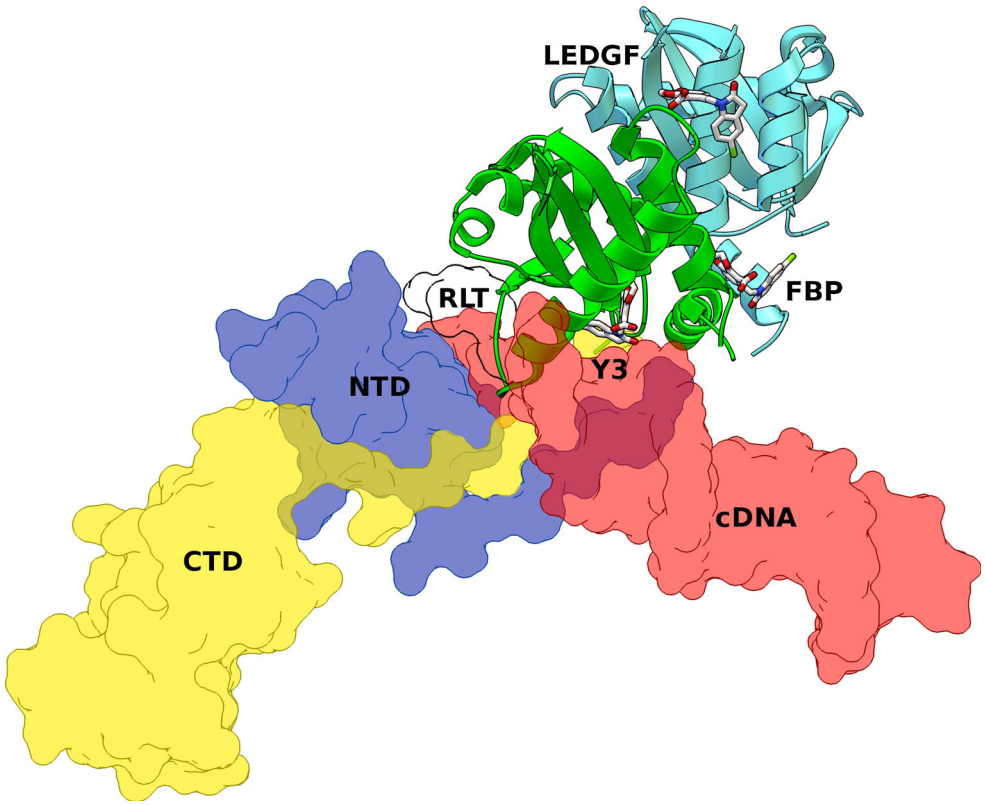


**Fig. 1** Integrase (IN) functional structure and architecture. The three domain structure of a monomer of IN is displayed. The PFV IN crystal structure (from 3OS1.pdb) of the "target capture complex" with DNA is displayed in surface mode, with the C-Terminal Domain in *yellow*, the N-Terminal Domain in *light blue*, and the human DNA in salmon. The 3NF8 reference structure of the HIV IN Catalytic Core Domain dimer was superimposed onto this PFV IN crystal structure, and its CCD is shown in ribbon mode (with one monomer in *green* and the other in *cyan*). The "CDQ" allosteric fragment from 3NF8 is displayed as sticks with white carbons to highlight the three allosteric sites of HIV IN that were part of the SAMPL4 challenge: LEDGF, Y3, and FBP. A *black outline* and the label RLT show the location of the active site of IN. Raltegravir (labeled as RLT) was extracted by superimposing the PFV IN crystal structure from 3OYA.pdb onto the 3OS1.pdb structure of PFV IN. During catalysis, HIV IN is present as a tetramer (i.e., a dimer of dimers)

Although the three advanced INSTIs were only recently developed, multi-drug-resistant mutants against which these inhibitors lose their potency have already appeared in clinical settings [1, 17, 45, 46, 55]. There are three main, independent pathways resulting in INSTI resistance, which involve mutations at positions Tyr143, Asn155, and Gln148 [55], all of which are within the catalytic active site region. Mutations at these positions, especially when combined with additional secondary mutations at other positions, cause extensive cross-resistance to both Raltegravir and Elvitegravir, and mutations involving Gln148 significantly decrease the susceptibility of HIV to all three advanced INSTIs [1, 17, 55]. The fact that HIV can quickly evolve drug resistance against these strand transfer active site inhibitors of IN highlights the urgent need to discover and develop new classes of drugs that bind to different sites and display new mechanisms of action.

### *Utility of allosteric inhibitors*

Combinations of two different classes of inhibitors that act on the same enzyme have been shown to inhibit broad panels of many different multi-drug-resistant mutants and to also decrease the probability of the emergence of new drug-resistant mutants, as exemplified by the combination of an active site inhibitor and an allosteric inhibitor of Bcr-Abl, a kinase target for cancer chemotherapy [25, 58]. This also appears to be the case for HIV treatment. When a Nucleoside Reverse Transcriptase Inhibitor (NRTI; NRTIs target the active site of HIV reverse transcriptase, or RT) is combined with an allosteric Non-Nucleoside Reverse Transcriptase Inhibitor (NNRTI; NNRTIs target a non-active site region of HIV RT), the evolution of drug resistance to both classes of drugs is impeded [10].

*LEDGF inhibitors*

One new class of inhibitors that seem particularly promising in the fight against AIDS are the subset of ALLosteric INtegrase Inhibitors (ALLINIs) called LEDGINs [7], which bind to the LEDGF site at the dimer interface of the CCD [12, 28]. LEDGF (for Lens Epithilial-Derived Growth Factor) is a human protein that HIV exploits: when IN interacts with LEDGF/p75, it guides the integration of the viral genome into the regions of our chromosomes where the actively expressed genes are located [4], which increases the probability of the subsequent production of viral proteins that can then help spread the infection. The LEDGINs use a carboxylate group to mimic a key interaction that LEDGF utilizes to bind to the backbone amino groups of Glu170 and His171, which are located in the LEDGF site of IN [28]. When LEDGINs bind the LEDGF site, they promote and stabilize higher-order multimers of IN and inhibit the catalytic process [6, 26, 27, 53].

Before the challenge began, the participants were informed that most of the SAMPL4 compounds were known to bind to (at least) the LEDGF site of IN, but some of the compounds were known to bind to at least one of the two additional allosteric sites of IN, which were referred to as the "FBP" site (for Fragment Binding Pocket) and the "Y3" site (see Fig. 1). Like the LEDGF site, the FBP site is also located at the dimer interface of the CCD of IN. There are two LEDGF sites per IN CCD dimer, two FBP sites per IN CCD dimer, and also two Y3 sites per IN CCD dimer. But the Y3 site is entirely contained within each monomer of the core domain and is located underneath the very flexible 140s loop (i.e., Gly140-Gly149). The top of the 140s loop flanks the active site region, and the composition, conformation, and flexibility of the 140s loop is known to be critical to IN activity [11, 18, 44]. Participants in the pose prediction challenge were given the hint that, if they were concerned about trying to predict the binding site, they might wish to focus their efforts on the LEDGF site, though most chose not to do so. This could have led to successful binding mode predictions in $\sim$52 of 55 cases considered.

## SAMPL challenge preparation and logistics

The experimental data for the IN portion of SAMPL4 is described in detail elsewhere in this issue [42]. It includes a set of inactive compounds which were not observed to bind via both crystallography and surface plasmon resonance (SPR), and a set of actives; together, these were used for the virtual screening component of SAMPL4. Additionally, crystal structures for some 57 of the actives were used for the pose prediction challenge. Accurate affinities were measured via SPR for 8 of these compounds, and these were used for the affinity prediction challenge.

For each portion of the challenge, participants were provided with a PDF of introductory material on the system prepared by Thomas S. Peat, which included a brief overview of the biological relevance, the different binding sites, and some references to previous published work from the same discovery project. This PDF is provided in the Supporting Information. In addition to this PDF, participants in each individual component received a further set of calculation inputs which will be described below.

The integrase portion of SAMPL4 was staged, so that participants must either complete or opt-out of virtual screening before going on to pose prediction, and complete or opt-out of pose prediction before going on to affinity prediction. This was done because inputs for the subsequent portions of the challenge would reveal all or part of the results from the earlier challenge components. In some cases, participants opted to conduct the whole challenge using *only* the inputs for the virtual screening challenge, and thus had no information about the identities of actual binders and/or structures when working on the affinity prediction and pose prediction challenges. This was primarily the case for submission IDs 535-540.

The SAMPL4 challenge was advertised via the SAMPL website (http://sampl.eyesopen.com) and e-mails to past participants, others in the field, and the computational chemistry list (CCL), beginning in January, 2013. The virtual screening portion of the challenge was made available via the SAMPL website April 1, 2013, and participants moved on to the other components once their screening results were submitted, or once they opted out. Submissions for all challenge components were due Friday, August 16. The challenge wrapped up with the SAMPL4 workshop on September 20 at Stanford University. Submissions were allowed to be anonymous, though we[1] received only three anonymous submissions from this portion of the challenge. Because of this, however, we typically refer to submissions by their submission ID (a three digit number) rather than by the authors' names.

### Pre-challenge preparation

The challenge organizers were provided with three main inputs to prepare the SAMPL4 challenge. First, we received a disk with raw crystallography data and refined structures for the majority of the compounds which were crystallized. Second, we received a spreadsheet describing

[1] The SAMPL4 challenge was designed, run and evaluated by the Mobley lab with some help from Kim Branson, so when this report uses the word "we" to refer to an action relating to challenge design, logistics, and analysis, it refers to these authors—specifically, Mobley, Branson, Su, Lim, Wymer, and Liu.

the active compounds, with SMILES strings, 2D structures, information about the density, and the location of the data on the disk. Third, we received a document containing images of the chemical structures of many inactive compounds. Fourth, we received a list of the molecules for which affinities were being measured precisely via SPR. Our pre-challenge preparation mainly involved turning this information into suitable inputs for predictions, and checking the data. Here, we used OpenEye unified Python toolkits [41] unless otherwise noted.

*Preparing inactives*

For the list of non-binders, since we had only compound identifiers and images of the 2D structures, we re-drew 2D structures of all of the non-binding compounds in Marvin Sketch [35] and then stored SMILES of these which were subsequently canonicalized and turned into 3D structures using the OpenEye toolkits [41] and Omega [22, 23]. Since this step involved manually drawing the structures, all structures drawn were inspected by two different people to check for accuracy.

*Preparing actives*

We also needed SMILES strings and 3D structures for all of the binders. SMILES strings were available both in the spreadsheet we were provided and on the disk, but these were not always consistent, and typically omitted stereochemistry information. We found that the most reliable route to getting this information was to pull the 3D ligand structures from the protein structures we were provided, then add protons and perceive stereochemistry information based on these structures. However, strain or other issues in the structures on occasion resulted in incorrect assignment of stereochemistry.

To deal with incorrect assignment of stereochemistry, we used OpenEye's Flipper module to enumerate all stereoisomers for each ligand, and with the Shape toolkit overlaid these onto the ligand structures pulled from the refined PDB files, automatically selecting the best-scoring shape overlay as the correct stereoisomer for cases with high shape similarity. Any alternate stereoisomer case where the shape Tanimoto score was within 0.1 of the best scoring shape overlay was flagged for additional manual inspection, although ultimately all structures were inspected manually. Based on manual examination of the shape overlays and electron densities in cases where there was any ambiguity, we concluded that the automatically assigned stereochemistry information was correct in every case except AVX17587, 38673, 38741, 38742, 38747, 38748, 38749, 38782, 38789, 101124, and GL5243-84. This seemed primarily to be because of poor-quality shape overlays in these cases, possibly due to ligand strain. Once we finished applying this procedure, we saved 3D structures of the correct stereoisomer of every ligand, as well as the isomeric SMILES string specifying stereochemistry information. In some cases our shape overlay work here actually resulted in a re-evaluation and potentially a re-refinement of the crystal structure, as discussed elsewhere [42].

*Stereoisomer enumeration*

In general, chiral compounds were tested as a mix of stereoisomers, so treating isomers as distinct compounds provides an opportunity to expand the list of inactive compounds. This is especially true for the inactive compounds, but even for the active compounds, if a given stereoisomer is not observed to bind, it means either that it does not bind, or it is much weaker than the stereoisomer which is observed to bind. Thus, for all compounds we enumerated all stereoisomers using Flipper and assigned them an isomer ID which was added to their ID. For example, for AVX38670, with two stereoisomers, these were labeled AVX38670_0 and AVX38670_1 and treated separately for the virtual screening and (when applicable) pose prediction challenges. The issue of whether or not to treat alternate (apparently non-binding) stereoisomers of actives as inactives will be discussed further below.

After generating or reading in isomeric SMILES strings for all compounds, we also cross-checked for duplicate compounds under the same or different identifiers and removed a number of such duplicates. In the OpenEye toolkits, there is a 1:1 correspondence between an isomeric SMILES string and a particular compound in its standard representation, so we expected that this would catch all duplicates. However, because of differences in how bonding was assigned prior to generating isomeric SMILES strings, some SMILES strings were generated from the Kekulé representation of molecules and some were not. These forms result in different isomeric SMILES strings, so some duplicates remained when we conducted the challenge and were only removed when we discovered this in post-analysis, as discussed below.

*Protonation state assignment*

By default, protonation/tautomer states for provided 3D structures for all compounds were assigned via the OpenEye toolkits using their "neutral pH model" predictor, though we did some additional investigation for pose prediction and affinity prediction, as noted below.

*Molecular dynamics re-refinement*

In the process of preparing for SAMPL, several structures were re-refined and in several cases resulted in substantial changes. We were concerned that we might miss other problem cases, and sought an automated procedure to identify cases where the binding mode might be questionable. Therefore, we took all refined structures and simulated them in the AMBER99SB-ILDN protein force field [33] with the AMBER GAFF [56] in GROMACS 4.6.2 for 110 ps of equilibration and another 100 ps of production, using protein protonation states assigned by MCCE. Equilibration was done gradually releasing restraints on the protein+ligand. Following this, we monitored root mean squared deviation (RMSD) over the course of the short production simulations and looked for cases where the ligand moved substantially away from its starting binding mode, by more than 3 Å ~RMSD. This flagged several cases as potentially problematic—AVX17558, AVX38749, and AVX38747. All three have a somewhat-floppy alkyl tail which in at least two of the cases has fairly poor density, which may be part of the issue. Re-refinement from our final structures from MD did not result in substantial improvement. Still, to us this suggests that closer scrutiny of these three may still be warranted. Particularly, in AVX17558 and AVX38747, there is some question as to the chirality. For AVX17558, there is some evidence in the density that both stereoisomers bind [43], while for AVX38747, it is not completely clear which stereoisomer fits the density best [43]. The remaining cases remained quite close to the crystallographic structure.

Virtual screening

In addition to the IN background PDF noted above, virtual screening participants were provided with a README file, a template for submitting their predictions, isomeric SMILES strings and 3D structures (in MOL2 and SDF format) for all stereoisomers of all compounds, and a reference protein/ligand structure in the form of a 3NF8_reference.pdb file—essentially, the PDB 3NF8 structure, aligned to the frame of reference we had chosen for the challenge. This 3NF8 structure was selected in part because it contains a bound ligand from the series studied here, and in part because this ligand is observed in all six binding sites (both copies of the LEDGF, Y3, and FBP sites). The README file contained information on what they were to submit, notes about the reference structure and the locations of the three sites, and a substantial hint—that "many (though by no means all) of the ligands bind in the LEDGF site, so if you like, you can focus on just that site and still do relatively well." We also included a disclaimer that the ligand protonation/tautomer states are provided "as is" and participants might wish to investigate these on their own. Submissions included a rank for each compound, a field indicating whether or not it was predicted to bind ("yes" or "no") and a confidence level ranging from 1 (low confidence) to 5 (very confident). These files are provided in the Supporting Information.

After the challenge, we found some issues with duplicate or incorrect compounds included in the virtual screening set. Specifically, we had to remove AVX17684m (or AVX17684-mod) because it was present in only some of the files which were distributed, and AVX17268_1 because it was incorrect. And only one member of each given set of duplicates was considered in analysis. Duplicates/replicates included (AVX17556, AVX17561, and GL5243-84), (AVX17557 and AVX17587), (AVX101125 and AVX62777), (AVX17285 and AVX16980), and (AVX17557 and AVX17587).

Pose prediction

In addition to the IN background PDF, pose prediction participants were provided with a README file, the reference structure described above, and SMILES strings and 3D structures (in MOL2 and SDF format) for all ligands, as in the case of the virtual screening challenge. The main differences here were that in this case, the compound list included only active compounds, and additional information in the README file. Particularly, the README file additionally added some additional pointers concerning protonation/tautomerization states. For this challenge portion, we used Epik, from Schrödinger, to enumerate possible protonation and tautomer states, and cross-compared the Epik predictions with those from OpenEye's QuacPac [41]. As a result, we highlighted compounds AVX17715, AVX58741, AVX38779-38789, and AVX-101118 to 101119 as having possible uncertainty in their protonation states, and GL5243-102 as having two possible tautomers on its five-membered ring, so these notes were provided in the README. The input files are provided in the Supporting Information.

Depending on the nature of their method, participants submitted either a 3D structure of the ligand in its predicted binding mode (relative to the 3NF8_reference.pdb structure provided), omitting the protein; or a 3D structure of the ligand-protein complex. In this challenge, our analysis focused only on the predicted binding modes relative to a static structure, so in cases where the full protein structure was submitted (i.e. for flexible protein methods), we scored binding modes based on an alignment onto the static reference structure.

For pose prediction, participants received SMILES strings for 58 compounds but 3D structures for 65

compounds because of a scripting error which resulted in some extra isomers being included in the 3D structures directory. So participants should have predicted binding modes for 58 compounds. However, several additional compounds had to be removed prior to analysis. Specifically, AVX17680 was removed because participants were provided with the wrong SMILES string and 3D structure because of a scripting error. Additionally, AVX101121 had a discrepancy between its SMILES string and its structure (differing by a methyl) apparently due to confusion about the original identity of the compound in the experiments, so this was removed prior to analysis. A similar thing happened with AVX-17543 on the computational end—participants were given an incorrect ligand SMILES and structure, and this had to be removed prior to analysis. Finally, AVX-17557 and AVX-17587 are actually the same compound, prepared as different salts. Thus the final number of compounds analyzed was 54.

### Affinity prediction

In addition to the IN background PDF, affinity prediction participants were provided with 3D structures of all 8 ligands (in MOL2 and SDF format), a README file, the refined crystal structures PDB format, MTZ format density files for the crystal structures, shape overlays of the ligands onto the crystallographic ligands (generated by the OpenEye Shape toolkit [41]), the refined crystal structure and ligand for the compound from the 3ZSQ structure, which was used as the control compound in SPR, and a text file template for submissions, which contained fields for the compound ID, the predicted binding free energy, the predicted statistical uncertainty, and the predicted model uncertainty. In this case, the README file highlighted minor issues with the electron density for AVX-17557 and for the aliphatic amino in AVX-38780, and an alternate rotamer for Leu102 in AVX40811 and AVX40812, as well as uncertainty in the protonation state of AVX38780.

## SAMPL analysis methods

In general, analysis was done using OpenEye's Python toolkits for working with molecules and structures, and Python/NumPy for numerical data. Matplotlib was used for plots.

### Virtual screening

Virtual screening performance was analyzed by a variety of relatively standard metrics, including area under the curve (AUC) and enrichment factor at 10 % of the database screened (EF10), as well as the newer Boltzmann-enhanced discrimination of receiver operating characteristic (BEDROC) [52]. We also made enrichment and ROC plots for all submissions. These were done using our own Python implementation of the underlying routines.

### Pose prediction

Here, we focused primarily on judging pose predictions via RMSD. We used two different evaluation schemes depending on how we handled cases with multiple copies of the ligand bound. Since IN is a dimer, there are two essentially symmetric copies of each binding site, for a total of 6 binding sites. These "symmetric" sites exhibit non-crystallographic symmetry (sequence symmetry) and are in some cases not quite symmetric. Typically, they in fact were refined separately. This introduced some complexities for judging pose prediction. Even if a ligand only occupied the LEDGF site, and a participant only predicted one binding mode, two RMSD scores were possible depending on how the prediction was superimposed onto the crystallographic structure. To compute both values, we rotate the crystal structure to the alternate possible alignment onto the reference structure (thus handling the non-crystallographic symmetry). Then, we compute the RMSD based on both the original alignment and the new alignment, and retain the best value as the score for this submission. This scenario of only a single predicted binding mode applied to the majority of submissions, though a minority of participants predicted multiple binding modes for some ligands, and a minority of ligands bound in other binding sites or exhibited multiple site binding. In these cases, additional RMSD values were possible. For example, if a participant predicted a ligand to bind to the LEDGF site, and actual binding was observed in both LEDGF sites and the Y3 site, we would obtain four different RMSD values. To handle this ambiguity, we chose to use two different scoring schemes, which we call "by ligand" and "by pose". In the "by ligand" scheme, we choose each submission's best RMSD value for each ligand, resulting in a total of 54 RMSD values. In the "by pose" scheme, each experimental binding site and mode (LEDGF, Y3, FBP) is scored separately and the best RMSD value is retained for each, resulting in a total of 112 RMSD values. Since most participants predicted only one binding mode per compound, this latter scheme penalizes submissions which miss binding to the additional sites in the case of multiple-site binding, while the former does not.

Our analysis here focuses only on scoring the best RMSD value of each submission for each ligand or pose. In general one might also be interested in knowing the worst RMSD. But since all but two participants here submitted only a single binding mode for each compound, the best and worst values are essentially identical for most submissions here.

To evaluate RMSD scores, we used a maximal common substructure search to match predicted ligand binding modes onto the crystallographic binding modes since this matching was not always obvious. Particularly, submissions used a variety of file formats, and not all submissions included ligand hydrogen atoms. Some submissions also altered atom naming conventions, meaning that the most straightforward approach of simply matching atoms by their names would not always work. Additionally, some ligands had internal symmetries (for example, a symmetric, rotatable ring) and participants should not be penalized for flipping symmetric groups. So, for each ligand or pose considered, we evaluated multiple maximum common substructure matches using the OpenEye Python toolkits, and took the match yielding the lowest RMSD. This approach simultaneously handled the issue of internal symmetry, together with variations in atom naming and protonation state.

In some cases, portions of ligands were relatively flexible and had only weak electron density. For example, a number of ligands had a floppy alkyl tail which was relatively poorly resolved but still included in the refined structures. We wanted to avoid penalizing participants for predictions which did not fit the model well in regions of weak density. Therefore, we manually inspected the electron density for all ligands and built a list of ligand heavy atoms which did not fall within the $2F_o - F_c$ density when contoured at $1\sigma$. This included C54 and N57 for AVX-17557; C42, C48, and N51 for AVX-17558; C18 for AVX17684m; C18 and O29 for AVX38672; N30, N31, C24 and C6 for AVX38741; N23, O30, C17, O27 and O25 for AVX38742; C25, C26, and O28 for AVX38743; C22 for AVX38747; C14, O31, C22, C25, and C26 for AVX38748; O32 for AVX38749; O1, O25, and O26 for AVX101140; and C20, C21, C22, and C23 for GL5243-84. These atoms were excluded from RMSD calculation, so in these cases only the portions of the ligands which did have good electron density were counted for scoring. In this case, since most submissions did relatively poorly at predicting binding modes, this consideration did not substantially alter RMSD values. However, we believe this procedure is in general good practice to avoid a scenario where one method appears better than another simply because it gives binding modes more consistent with those from refinement, even when there is no difference in how well they fit the electron density.

We had originally planned to also calculate the diffraction-component precision index (DPI), and thus the coordinate error, for each of the structures [3]. This would provide a mechanism to compute the best achievable RMSD values. For example, two methods can be considered equally good whenever they yield the lowest RMSD which can be obtained given the coordinate error. Or, to put it another way, RMSD comparisons are useful only for RMSD values above the fundamental limit imposed by the precision in the coordinates. Experimental structures with very precise coordinates can permit RMSD comparisons down to very low values, while less precise structures provide less information about which predictions are the most accurate. This could be dealt with in analysis by assigning a DPI-adjusted RMSD to any submission which coincidentally obtained an RMSD value lower than the best possible value expected given the coordinate error. In general, we believe this approach is the correct one to take in comparing binding mode predictions by RMSD. However, we ran out of time to conduct this analysis prior to SAMPL, and here, so many binding modes proved very difficult to predict that small adjustments to the RMSD values for a few submissions on a few ligands would not have substantially affected the overall analysis.

One other metric commonly used to assess binding mode prediction is the fraction of ligands correctly predicted. However, "correct" is typically defined with respect to an arbitrary cutoff—for example, ligands predicted better than 2 Å ~RMSD might be said to be correctly predicted, while another practitioner might use a different cutoff. To avoid this ambiguity here, for each submission, we plotted the fraction of ligands correctly predicted as a function of RMSD cutoff $x$ and evaluated the area under the curve (AUC). These plots and the AUC were provided to participants and are discussed below. In general, a method will predict no binding modes correctly at a cutoff of 0 Å ~RMSD, and all binding modes correctly at a cutoff larger than the size of the receptor, with the fraction correct varying in between these. A reasonable AUC can be achieved in multiple ways—for example, by having many very accurate predictions but also many very wrong predictions, or by having all predictions achieve modest accuracy.

As noted above in Section 2.1.5, there may still be questions about the true ligand binding mode or bound structure in a handful of cases. However, the set is large enough that these cases do not substantially affect the conclusions of the analysis here, and so our overall analysis includes these cases.

It is worth noting that the vast majority of the ligands in this series bind exclusively in the LEDGF site, with a smaller number exhibiting multiple site binding, and a few binding only in alternate sites. Specifically, AVX-15988, AVX-17389, and AVX-17679 bind FBP exclusively; and AVX-17631 binds both the LEDGF site and the FBP. pC2-A03 binds just one of the Y3 sites, and AVX-17258 and AVX-101140 bind both Y3 and the LEDGF site. A few structures are annotated with other possibilities—AVX-17260 is noted to have some density in the FBP, but is only modeled in the LEDGF site; and AVX-17285 is suggested

to perhaps have multiple conformations but only one is modeled.

This analysis focused on ligand binding mode prediction essentially in the absence of protein motion, and even in cases where participants used a flexible protein and submitted a protein structure along with the ligand binding mode, this was used only to align their protein structure onto the reference structure used for judging. We made this choice primarily because protein motion here was quite minor, with side-chain rearrangements only appearing in a handful of cases (for example, LEU102 for AVX-17377, AVX-40811, and AVX-40812) and GLU157 in pC2-A03 and AVX-17377), and more substantial protein motion appeared to in general be absent. Thus it seemed appropriate to focus this SAMPL primarily on ligand binding mode prediction within an essentially static protein structure.

Because binding site prediction was a substantial challenge which was here convoluted with binding mode prediction, we recomputed all metrics for each submission for the fraction of poses which were placed "in" the correct binding site. For the purposes of this analysis, we considered compounds in the correct binding site when they were placed so that the predicted center-of-mass (COM) location is nearer the COM of a ligand in that binding site in the 3NF8 structure than the COM of the ligand in any other binding site. In other words, each ligand was considered to be in the binding site its center-of-mass was nearest to.

We also computed an interaction fingerprint metric to look at whether predicted binding modes made the correct contacts with the protein. Interaction fingerprints were computed using Van der Waals (VdW) interactions from the DOCK 3.5 scoring function [13], and the hydrogen bonding term from SCORE [57]. For each atom in the protein the VdW and hydrogen bonding interactions were checked against every atom in the ligand. A bit string was constructed for each atom in the protein. Protein atoms with a favorable VdW or hydrogen bonding interactions had their bits set to 1 otherwise 0. A bit string was calculated for the crystallographic ligand coordinates (the reference string) and the docked poses. The Tanimoto coefficient was used to assess the similarity in protein contacts between the reference and docked poses.

Several minor changes were made to structures after the SAMPL challenge and all analysis was completed, during the process of deposition to the PDB. Because these changes were made at such a late date, when many SAMPL manuscripts were already in review and/or accepted for publication, our analysis was left as is and these updates are only noted here. Specifically, further work on AVX-38743 determined that a mixed regio-isomer is actually a better fit to the density, as seen in the final structure (PDB 4CF9). And for AVX-38741, it was determined that a ring which had been thought to have formed within the molecule in fact did not form, altering the compound identity (PDB 4CF8).

## Affinity prediction

Of the actual binders observed here by crystallography, only a small number were strong enough to obtain accurate affinities via surface plasmon resonance (SPR). Affinities measured by SPR were provided for 8 compounds by Peat et al. [42]. These were provided as $K_d$ values with uncertainties and converted to $\Delta G^\circ$ for analysis. A couple of additional compounds were also available, but due to questions about the stoichiometry of binding and other issues these were excluded from the analysis. Final

**Table 1** Calculated metrics for SAMPL4 virtual screening submissions

| ID | BEDROC | AUC | EF (10 %) |
|---|---|---|---|
| 007 | 0.20 ± 0.07 | 0.53 ± 0.04 | 1.07 ± 0.37 |
| 008 | 0.37 ± 0.09 | 0.63 ± 0.04 | 1.97 ± 0.48 |
| 133 | 0.13 ± 0.05 | 0.59 ± 0.04 | 1.07 ± 0.39 |
| 134 | 0.20 ± 0.07 | 0.62 ± 0.04 | 1.25 ± 0.40 |
| 135 | 0.37 ± 0.09 | 0.64 ± 0.04 | 2.21 ± 0.51 |
| 136 | 0.27 ± 0.08 | 0.65 ± 0.04 | 1.47 ± 0.43 |
| 146 | 0.20 ± 0.07 | 0.56 ± 0.04 | 1.25 ± 0.39 |
| 147 | 0.28 ± 0.08 | 0.55 ± 0.05 | 1.79 ± 0.46 |
| 148 | 0.36 ± 0.09 | 0.59 ± 0.04 | 1.61 ± 0.45 |
| 157 | 0.14 ± 0.07 | 0.45 ± 0.04 | 0.72 ± 0.32 |
| 164 | 0.56 ± 0.09 | 0.71 ± 0.04 | 3.22 ± 0.49 |
| 165 | 0.20 ± 0.06 | 0.55 ± 0.04 | 1.43 ± 0.44 |
| 171 | 0.38 ± 0.10 | 0.60 ± 0.04 | 1.25 ± 0.41 |
| 172 | 0.24 ± 0.07 | 0.54 ± 0.04 | 1.43 ± 0.42 |
| 173 | 0.18 ± 0.06 | 0.49 ± 0.05 | 1.25 ± 0.41 |
| 174 | 0.20 ± 0.07 | 0.49 ± 0.05 | 1.07 ± 0.39 |
| 175 | 0.11 ± 0.05 | 0.45 ± 0.04 | 0.72 ± 0.32 |
| 176 | 0.10 ± 0.05 | 0.46 ± 0.05 | 0.36 ± 0.26 |
| 198 | 0.13 ± 0.06 | 0.52 ± 0.04 | 0.72 ± 0.34 |
| 200 | 0.14 ± 0.07 | 0.48 ± 0.04 | 0.54 ± 0.29 |
| 238 | 0.14 ± 0.07 | 0.50 ± 0.04 | 0.72 ± 0.34 |
| 239 | 0.19 ± 0.07 | 0.56 ± 0.04 | 1.07 ± 0.38 |
| 240 | 0.20 ± 0.07 | 0.53 ± 0.04 | 1.25 ± 0.41 |
| 241 | 0.16 ± 0.06 | 0.54 ± 0.04 | 0.89 ± 0.36 |
| 242 | 0.16 ± 0.06 | 0.56 ± 0.04 | 0.89 ± 0.38 |
| 524 | 0.11 ± 0.05 | 0.48 ± 0.04 | 0.72 ± 0.34 |
| 546 | 0.20 ± 0.07 | 0.56 ± 0.04 | 1.25 ± 0.41 |
| 547 | 0.20 ± 0.07 | 0.57 ± 0.04 | 1.25 ± 0.39 |

Also shown are control or null models 007 and 008. For each submission ID, we computed the area under the enrichment curve (AUC), the Boltzmann-enhanced discrimination of receiver operating characteristic (BEDROC), and the enrichment factor at 10 %. For this set, the maximum enrichment factor at 10 % is 305/56 = 5.45

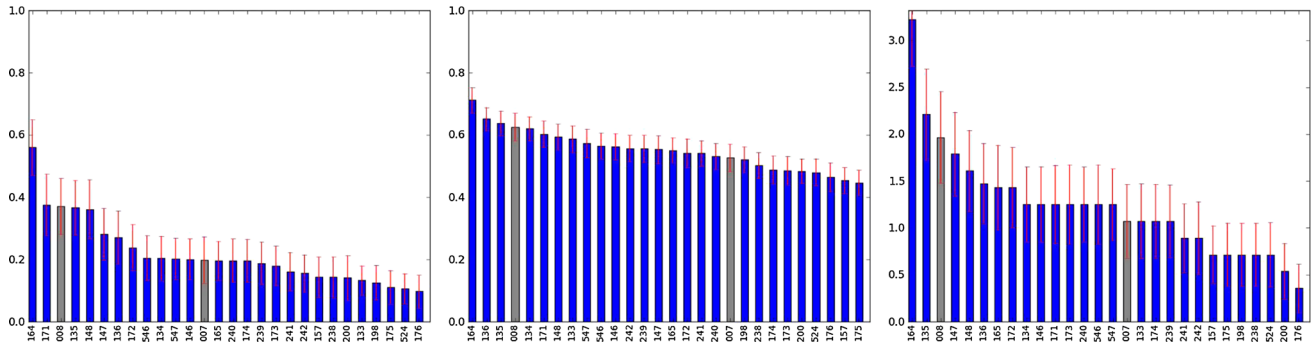

**(a)** BEDROC **(b)** AUC **(c)** EF 10%

**Fig. 2** Calculated metrics for SAMPL4 virtual screening statistics, graphed in ranked order. The statistics are as given in Table 1. Note that many submissions have overlapping *error bars*, so ranked order is not necessarily indicative of *significantly* better performance

affinities are all fairly weak, spanning from 200 to 1,460 μM, unfortunately giving a rather narrow range of binding free energies.

All submissions were analyzed by a variety of standard metrics, including average error, average unsigned error, RMS error, Pearson correlation coefficient (R), and Kendall tau, as well as the slope of a best linear fit of calculated to predicted values. Additionally, we compared the median Kullback–Leibler (KL) divergence for all methods, adjusted to avoid penalizing for predicted uncertainties that are smaller than the experimental error when the calculated value is close to the experimental value, as discussed in more detail elsewhere in this issue [37]. Because KL divergences are difficult to average when performance is poor, we also looked at the expected loss, given by $L = <1 - e^{-(KL)}>$ where $KL$ is the KL divergence [37].

We also examined one additional metric, what we call the error slope, which evaluates how well submissions predicted uncertainties. This looks at the fraction of experimental values (resampled with noise drawn from the experimental distribution) falling within a given multiple of a submissions assigned statistical uncertainty, and compares it to the fraction expected (a Q–Q plot), as discussed elsewhere in this issue [37]. A line is fit to this, and a slope of 1 corresponds to accurate uncertainty estimation; a slope higher than 1 means uncertainty estimates were too high on average, and a slope lower than 1 means uncertainty estimates were too low on average.

### Error analysis

For all sections of the challenge, we computed uncertainty estimates in all numerical values as the standard deviation measured over a bootstrapping procedure as explained in more detail elsewhere in this issue [37]. Some additional detail is warranted for the virtual screening analysis, where bootstrapping consisted of constructing "new" datasets by selecting a new set of compounds of the same length at random from the original set, with replacement, and pairing these with the corresponding predicted values. This new set typically contained multiple entries of some compounds and omitted others, allowing assessment of the dependence of the computed results on the set. As usual, the uncertainty was reported as the standard deviation over 1,000 bootstrap trials.

## Integrase screening results

### SAMPL analysis focused on the full set

For the binding prediction portion of the challenge, we received 26 submissions from nine different research groups. Overall statistics for these are shown in Table 1 and Fig. 2. We also show statistics for two control or null models, 007 and 008, described below. In general, this portion of the challenge was extremely challenging, and even the best methods enriched actives only slightly better than random over the entire set of 305 compounds (with 249 non-binders).[2] We attribute this to several factors. First, participants did not know the actual binding site, increasing the potential for false positives. Second, the inactive compounds here are available precisely because they were thought to be good candidate binders and therefore were tested experimentally. That is, they are part of the same series as the active compounds and resemble the active compounds in essentially every respect. Third, many (116) of the inactives are in fact alternate stereoisomers of active compounds, further increasing their resemblance to actives. The challenging nature of this test can be observed by noting that only five submissions (submission IDs 134, 135, 136, 164, and 171) achieved an

[2] The challenge began with 322 compounds, 260 non-binders, and 62 binders, but due to errors and redundancies, final analysis was run on 305 compounds and 56 binders.

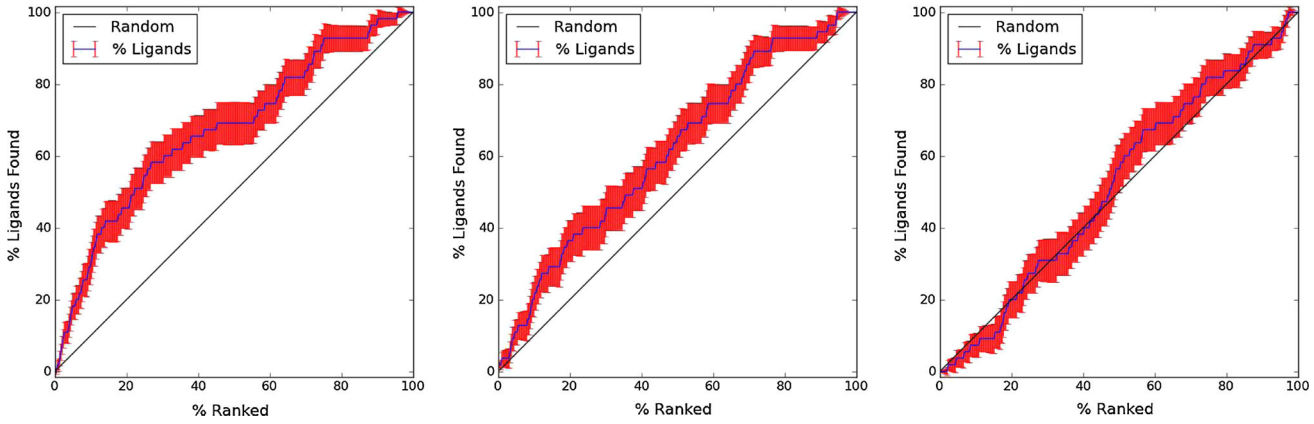


**(a)** Enrichment, 164 **(b)** Enrichment, 135 **(c)** Enrichment, 198

**Fig. 3** Enrichment plots for two of the best-performing virtual screening submissions, and one for which performance is close to random. Submission 164 was the top performer by all metrics, and 135 was one of the other top performers. 198 is shown here as representative of more typical performance for comparison. *Error bars* are shown in *red* and give an idea of the expected variation with the composition of the set

AUC of 0.6 or higher (predicting active compounds at random would be expected to yield an AUC of 0.5), and only six (IDs 135, 136, 147, 148, 164, and 172) achieved an enrichment factor at 10 % (EF) more than one standard error better than random (1.0). Enrichment plots for two of the top submissions (164, which is top by every metric, and 135, which is consistently among the top) are shown in Fig. 3, along with an enrichment plot for a more typical submission (198).

Submission 164 was the top performer by every metric, and really stood out from the pack, especially in terms of early enrichment, so it is worth examining the approach in slightly more detail, but we refer the reader elsewhere for a full description [54]. In brief, this submission came from a human expert with more than 10 years experience working on this specific target. The specific procedure used docking with GOLD, then a pharmacophore search done in MOE using many crystallographic structures of LEDGF ligands to generate the query. MOE and an electrostatic similarity search were used for filtering. The correct stereochemistry of binders was assigned manually after electrostatic similarity comparison and binding mode examination. Overall, screening via this approach involved substantial manual intervention and expert knowledge. It is worth highlighting that this approach did especially well at early enrichment, with an enrichment factor of $3.2 \pm 0.5$. The maximum EF at 10 % on this set is 5.2. The observation that the top performing submission used substantial manual intervention and human expertise echoes the conclusion of SAMPL2, where human experts outperformed automated methods at pose prediction [47].

Submission 135 was also particularly interesting, in that it began from essentially the same inputs as 133 and 134—AutoDock/Vina docking calculations—but used BEDAM alchemical binding free energy calculations [5, 16] to score predictions. This appears to have been remarkably successful at improving recognition of LEDGF binders, and was hampered by time constraints—not all molecules could be analyzed in this way, so apparently many of the actives which were still missed lacked binding free energy estimates. We refer the reader elsewhere in this issue for additional discussion of this submission [15].

Overall, we saw submissions using a fairly wide range of other methods, though in general most of these were relatively rapid methods (with the exception of 135) involving at least some component of docking. A variety of submissions used simple docking with various packages and different target protein structures (133, 157, 198, 200, 238, 239–242, 524, 546–547) and most others used docking plus something else (i.e. rescoring, scoring function modifications, etc.). For example, as discussed, 135 used docking plus alchemical free energy calculations, while 136 used a consensus score of 133–135, 146–148 used WILMA docking plus SIE re-scoring, 165 used protein-specific charges, and so on. 172–176 stood out from other approaches because they used a pharmacophore docking approach. However, in general among these methods, we do not see an approach which clearly stands out from the rest.

We also ran two control or null models, submissions 007 and 008, which were not formally SAMPL submissions. ID 007 is based on molecular weight alone—compounds are ranked simply based on molecular weight, with heavier compounds predicted to bind best. ID 008 is based on ligand shape similarity, computing using OpenEye's ROCS, with reference ligand CDQ 225 from the 3NF8

**Table 2** Statistics for SAMPL4 pose prediction

| ID | By ligand | | | By pose | | | Correct site, by ligand | | |
|---|---|---|---|---|---|---|---|---|---|
| | $\overline{RMSD}$ | Med. *RMSD* | AUC | $\overline{RMSD}$ | Med. *RMSD* | AUC | $\overline{RMSD}$ | Med. *RMSD* | AUC |
| 143 | 6.5 ± 1.0 | 3.8 ± 0.4 | 93.4 ± 1.0 | 7.2 ± 0.8 | 4.1 ± 0.4 | 92.7 ± 0.8 | 3.4 ± 1.0 | 3.4 ± 0.4 | 96.5 ± 1.0 |
| 154 | 12.2 ± 1.7 | 4.4 ± 4.7 | 87.7 ± 1.7 | 13.0 ± 1.2 | 4.9 ± 4.7 | 86.9 ± 1.2 | 2.3 ± 1.7 | 1.5 ± 4.7 | 97.6 ± 1.7 |
| 155 | 15.4 ± 1.5 | 17.2 ± 5.5 | 84.5 ± 1.5 | 15.8 ± 1.1 | 20.0 ± 4.1 | 84.1 ± 1.1 | 3.8 ± 1.5 | 1.8 ± 5.5 | 96.1 ± 1.5 |
| 156 | 7.8 ± 0.9 | 5.8 ± 1.0 | 92.1 ± 0.9 | 8.6 ± 0.7 | 6.2 ± 0.8 | 91.3 ± 0.7 | 6.7 ± 0.9 | 5.2 ± 1.0 | 93.2 ± 0.9 |
| 177 | 5.6 ± 0.9 | 4.0 ± 0.4 | 94.3 ± 0.9 | 6.4 ± 0.7 | 4.1 ± 0.2 | 93.5 ± 0.7 | 3.3 ± 0.9 | 3.7 ± 0.4 | 96.6 ± 0.9 |
| 300 | 20.4 ± 1.1 | 18.7 ± 0.4 | 79.5 ± 1.1 | 20.4 ± 0.7 | 18.9 ± 0.3 | 79.5 ± 0.7 | 23.2 ± 1.1 | 17.5 ± 0.4 | 76.7 ± 1.1 |
| 301 | 4.3 ± 0.8 | 2.8 ± 0.4 | 95.6 ± 0.8 | 5.3 ± 0.7 | 2.8 ± 0.3 | 94.6 ± 0.7 | 2.8 ± 0.8 | 2.5 ± 0.4 | 97.1 ± 0.8 |
| 535 | 22.6 ± 0.8 | 24.0 ± 0.3 | 77.3 ± 0.8 | 22.7 ± 0.5 | 24.0 ± 0.2 | 77.2 ± 0.5 | 3.4 ± 0.8 | 3.3 ± 0.3 | 96.5 ± 0.8 |
| 536 | 6.3 ± 0.7 | 4.8 ± 0.4 | 93.6 ± 0.7 | 7.2 ± 0.6 | 4.9 ± 0.3 | 92.7 ± 0.6 | 5.0 ± 0.7 | 4.7 ± 0.4 | 94.9 ± 0.7 |
| 537 | 26.7 ± 0.9 | 28.8 ± 0.6 | 73.2 ± 0.9 | 26.9 ± 0.6 | 28.6 ± 0.4 | 73.0 ± 0.6 | 6.3 ± 0.9 | 6.3 ± 0.6 | 93.5 ± 0.9 |
| 538 | 26.1 ± 1.1 | 28.1 ± 0.5 | 73.8 ± 1.1 | 26.3 ± 0.7 | 28.1 ± 0.3 | 73.6 ± 0.7 | 5.2 ± 1.1 | 5.1 ± 0.5 | 94.7 ± 1.1 |
| 539 | 27.3 ± 1.0 | 29.2 ± 0.5 | 72.6 ± 1.0 | 27.4 ± 0.6 | 29.0 ± 0.3 | 72.5 ± 0.6 | 5.5 ± 1.0 | 6.2 ± 0.5 | 94.4 ± 1.0 |
| 540 | 27.0 ± 0.9 | 29.1 ± 0.4 | 72.9 ± 0.9 | 27.2 ± 0.6 | 29.0 ± 0.3 | 72.7 ± 0.6 | 5.5 ± 0.9 | 6.2 ± 0.4 | 94.4 ± 0.9 |
| 583 | 25.7 ± 1.6 | 24.3 ± 2.7 | 74.2 ± 1.6 | 26.0 ± 1.1 | 25.3 ± 1.8 | 73.9 ± 1.1 | 13.5 ± 1.6 | 14.1 ± 2.7 | 86.4 ± 1.6 |
| 1,000 | 20.7 ± 1.4 | 24.4 ± 0.8 | 79.2 ± 1.4 | 20.9 ± 0.9 | 24.4 ± 0.4 | 79.0 ± 0.9 | 4.0 ± 1.4 | 4.5 ± 0.8 | 95.9 ± 1.4 |

Statistics by ligand (where the lowest RMSD prediction is taken for each ligand), by pose (where the lowest RMSD prediction is considered separately for each experimental binding mode), and by ligand for only the fraction of ligands placed into (or nearest) the correct binding site

reference structure. This approach, shape similarity to a known ligand, is actually quite reasonable and should be thought of as a control rather than a null model. Indeed, we find that many methods outperform 007, which does not do significantly better than random at recognizing actives. On the other hand, 008, based on shape similarity to a known ligand, performs quite well, and indeed is among the top methods in terms of early enrichment and is one of the approaches achieving an AUC over 0.6.

Post-SAMPL: alternate isomers may not be non-binders

We constructed the virtual screening set with the assumption that alternate isomers of binders are in fact non-binders, but this may in fact be an oversimplification. This approach seemed reasonable initially, since SPR and crystallography were typically run on mixtures of isomers, so isomers which were not observed to bind crystallographically are at least much weaker binders than the binding isomer. But this does not guarantee that they are actually non-binders. Consider a hypothetical molecule $A$ with isomers $A_0$ and $A_1$, where $A_0$ has a dissociation constant of 5 μM and $A_1$ has a dissociation constant of 100 μM. Binding of $A_1$ is sufficiently weaker than $A_0$ that it would be extremely difficult to detect in an assay on an equal mixture of the two isomers, and hence would be labeled a "non-binder". Hence, it would perhaps be more appropriate to divide our virtual screening set into three categories: "actives", "inactives", and "inactives or very weak actives". Success in the last category would require a method to rank these compounds lower than the corresponding alternate isomers which are in the "actives" category. In any case, this analysis suggests that a re-analysis of the SAMPL results may be needed.

In view of this uncertainty, we ran a re-analysis of the virtual screening challenge on a new set which dropped all alternate isomers of active compounds, effectively excluding the "inactive or very weak active" category and retaining only true actives and inactives. This reduced the number of compounds analyzed from 305 to 189, while retaining the same 56 actives. Full statistics and plots for this subset are provided in the Supporting Information. Overall, the ranking of methods by our different metrics stayed somewhat similar in many cases, though the best BEDROC values rose very substantially, indicating better early enrichment. Also, submission 547, which had been essentially in the middle by every metric instead jumped to second place by every metric, in some cases within error of our best submission, 164. In our view the marked change in performance here suggests that some fraction of the inactive compounds may in fact be weak actives. Additionally, this observation has obvious implications for future experimental design and design of SAMPL challenges, since it means additional information is needed to distinguish between very weak actives which are tested together with stronger actives, versus true non binders.

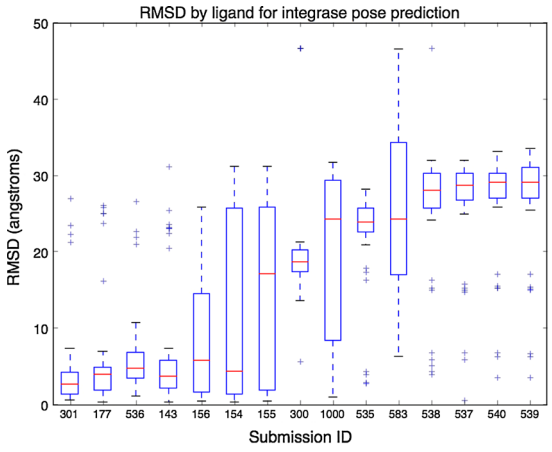


**(a)** RMSD

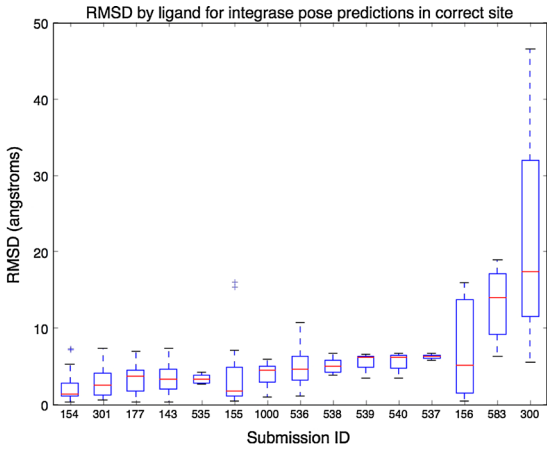


**(b)** RMSD, correct site

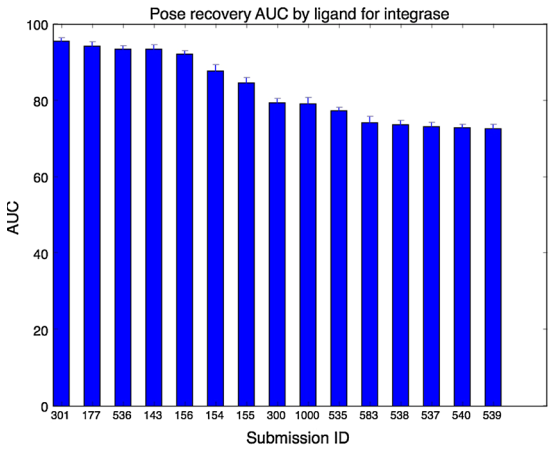


**(c)** AUC

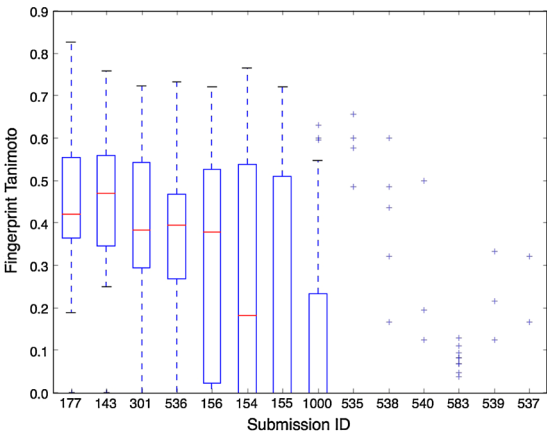


**(d)** Fingerprint Tanimoto

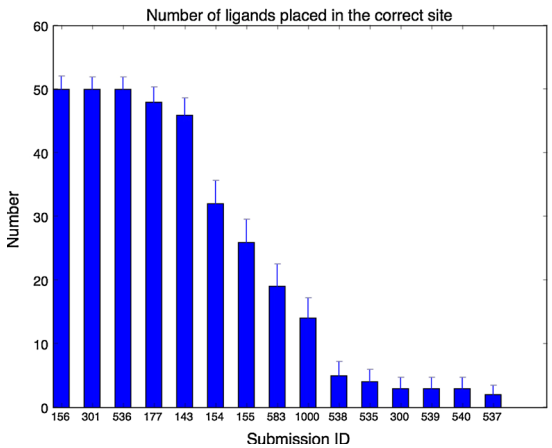


**(e)** Site identification

**Fig. 4** Ranked performance on pose prediction, by various metrics. **a**, **b**, *box/whisker plots* showing performance by ligand as judged by RMSD; **b** focuses only on the subset of ligands placed within the correct site. **c** performance judged by AUC, by ligand; and **d** performance by ligand as judged by interaction fingerprint Tanimoto scores. **e** The number of ligands placed into the correct binding site for each submission. For *bar plots*, normal submissions are shown in *blue*, while control models (300, 301) are shown in *gray*, as discussed in the text

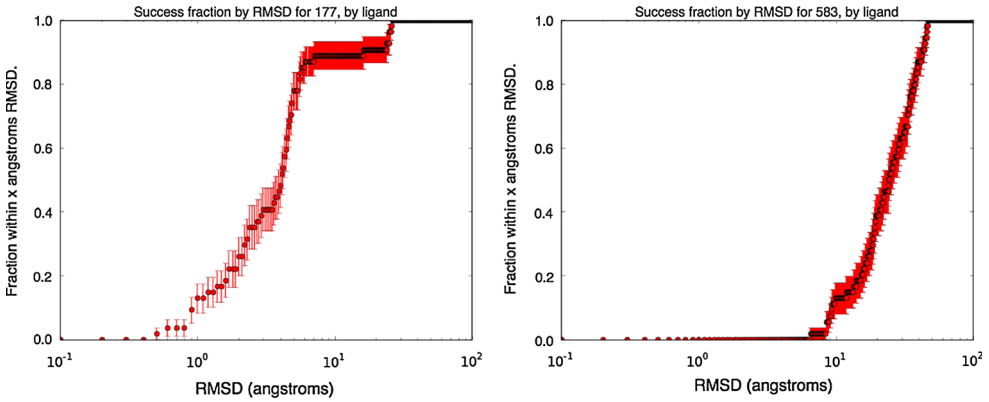


**(a)** 177 **(b)** 583

**Fig. 5** Fraction of ligands with correct binding modes, versus RMSD cutoff. Shown are the fraction of ligand binding modes predicted correctly within a cutoff of $x$ Å RMSD, where $x$ is the *horizontal axis*. The scale is semi-log. Method 177 performed particularly well by this and other metrics, while 583 did not perform particularly well here. In submission 177, most ligands are predicted correctly within 10 Å RMSD, with a substantial fraction better 3 Å. In contrast, in 583, only a small number are predicted better than ~10 Å RMSD

## Integrase pose prediction results

Pose prediction participation was, from our perspective, surprisingly light. We received 12 submissions from five research groups. While in principle participants could submit multiple predicted binding modes for each ligand (since some ligands bound in multiple sites, completely successful predictions would have needed to do so), only three submissions did so, and in only a few cases. As noted above, we score each method both by the best predicted pose for each ligand, and by the best predicted pose for each experimental binding mode. Since a number of ligands have multiple binding modes, the latter is a substantially longer set.

Our initial analysis focused primarily on examining the RMSD for each submission, as shown in Table 2 and Fig. 4. Because RMSD is unbounded, a simple mean is not necessarily a good metric overall, so we also looked at the median RMSD. As discussed in the analysis section above, we also wanted to look at how often binding modes were predicted successfully, but without an arbitrary "success" RMSD threshold. So instead, we computed the area under the curve (AUC) for the fraction of poses predicted correctly at a given cutoff level; here, a higher number is better.

As Fig. 4 shows, each method had substantial variability in performance. While the top methods tended to predict more poses correctly, no method predicted all binding modes to high accuracy, as seen by RMSD. The figure focuses on the best predictions for each ligand, but a similar conclusion holds for predictions when judged by pose, as shown in the Supporting Information. Still, by a variety of metrics, submissions 177, 536, 143, and 154 were typically among the top performers. Test submission 301 also did quite well, and is a reference model we ran internally and will be discussed below. ID 177 used XP Glide [14] with rescoring via DrugScore and MM-PB/SA [29], and 143 used AutoDock Vina [51], while ID 154 used Wilma docking and SIE re-scoring [38, 48]. ID 536 used DOCK 3.7. All of these except submission 536 considered binding to multiple sites.

Our AUC metric assesses what fraction of pose predictions were successful as a function of the definition of success (RMSD cutoff). RMSD has at least one major disadvantage, in that it is unbounded, so a method which performs modestly well on 25 compounds and very poorly on 30 could actually appear worse (by average RMSD) than a method which performs fairly poorly on all 55, simply because very large RMSD values can contribute so much to the average. In contrast, AUC is relatively insensitive to failures and particularly sensitive to the fraction of binding poses correctly identified. Sample plots of the data which goes into the AUC calculation are shown in Fig. 5. The plot uses a semi-log scale, and clearly shows how submission 177 performs substantially better than 583 in terms of pose prediction success.

Our fingerprint Tanimoto metric focuses on whether poses identified the correct interactions and contacts with the protein, rather than on reproducing the experimental binding mode precisely. Thus, this is a more flexible criteria for success within the binding site, though it rapidly goes to zero as the predicted binding mode moves away from the true binding site. The top methods seem to have substantial success, typically, at identifying the correct interactions, and a number of submissions perform nearly as well by this metric and are probably statistically indistinguishable.

Some insight into why methods had such a broad range of performance can be gained by examining Fig. 4c, which looks only at the fraction of ligands placed into the correct

**Table 3** Statistics for IN affinity prediction

| ID | Avg. Err. | RMS | AUE | Tau | R |
|---|---|---|---|---|---|
| 012 | −18.0 ± 0.1 | 18.0 ± 0.1 | 18.0 ± 0.1 | −0.2 ± 0.0 | −0.2 ± 0.0 |
| 013 | −41.6 ± 2.5 | 42.2 ± 2.8 | 41.6 ± 2.5 | −0.4 ± 0.0 | −0.6 ± 0.0 |
| 182 | −3.8 ± 0.3 | 3.9 ± 0.3 | 3.8 ± 0.3 | −0.4 ± 0.3 | −0.7 ± 0.3 |
| 183 | −3.2 ± 0.3 | 3.3 ± 0.3 | 3.3 ± 0.3 | −0.6 ± 0.2 | −0.8 ± 0.2 |
| 184 | −1.2 ± 0.5 | 1.8 ± 0.4 | 1.3 ± 0.4 | −0.1 ± 0.3 | −0.3 ± 0.3 |
| 190 | −2.2 ± 0.8 | 3.1 ± 0.5 | 2.7 ± 0.5 | −0.1 ± 0.2 | −0.2 ± 0.3 |
| 191 | −3.8 ± 0.3 | 4.0 ± 0.3 | 3.8 ± 0.3 | 0.2 ± 0.3 | 0.4 ± 0.3 |
| 199 | −22.2 ± 4.2 | 25.1 ± 2.8 | 23.0 ± 3.6 | 0.6 ± 0.3 | 0.6 ± 0.4 |
| 201 | −25.1 ± 5.0 | 28.8 ± 2.8 | 27.1 ± 3.4 | 0.5 ± 0.3 | 0.6 ± 0.4 |
| 233 | −24.6 ± 4.8 | 28.1 ± 2.6 | 26.6 ± 3.3 | 0.4 ± 0.3 | 0.5 ± 0.4 |
| 234 | −25.6 ± 4.4 | 28.5 ± 2.8 | 26.5 ± 3.7 | 0.2 ± 0.3 | 0.5 ± 0.4 |
| 235 | −17.4 ± 3.6 | 20.1 ± 2.5 | 18.2 ± 3.1 | 0.5 ± 0.3 | 0.6 ± 0.3 |
| 236 | −17.5 ± 3.4 | 20.0 ± 1.9 | 18.9 ± 2.4 | 0.4 ± 0.3 | 0.6 ± 0.4 |
| 237 | −27.0 ± 3.4 | 28.6 ± 2.7 | 27.0 ± 3.4 | 0.2 ± 0.3 | 0.5 ± 0.4 |
| 549 | −7.8 ± 1.3 | 8.6 ± 1.3 | 7.8 ± 1.3 | −0.2 ± 0.3 | −0.3 ± 0.3 |

The average error, RMS error, AUE, Kendall tau, and Pearson R

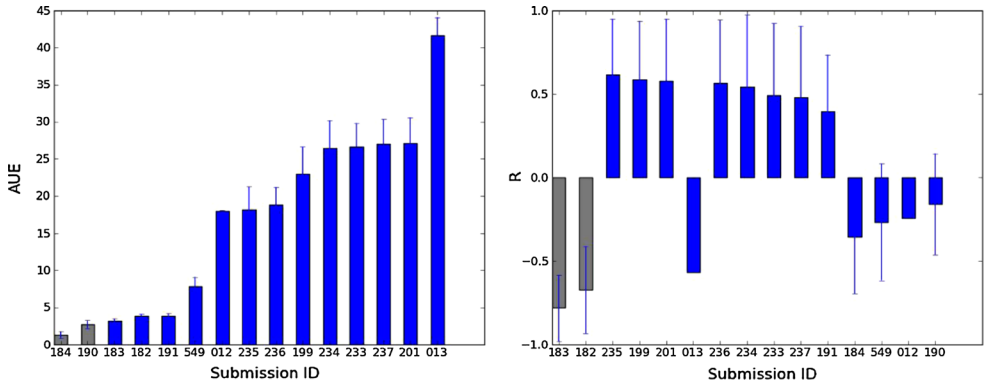


**(a)** Ranked AUE **(b)** Ranked R

**Fig. 6** Representative statistics for the integrase affinity challenge. Shown are the Pearson correlation coefficient, *R*, and the average unsigned error (AUE). Normal submissions are shown in *blue*; control models are shown in *gray*, as discussed in the text

binding site. Since most methods considered all three binding sites, many of the high RMSD predictions were a result of predicting the wrong binding site. Thus, performance seems more comparable across methods when considering only poses within the correct site. However, it is worth noting that the same submissions are still among the top performers. This is further highlighted by looking at the number of ligands placed into the correct site, in Fig. 4f. Despite the hint given participants that they could focus primarily on the LEDGF site, most chose to include both the Y3 and FBP sites when making predictions, as well, and so the majority of submissions typically selected the incorrect binding site. However, of the top submissions, most *did* include multiple sites in their analysis. The fact that several submissions were thus fairly successful at identifying the correct binding site is encouraging.

Submissions 300 and 301 are an attempt at generating null or comparison models. Thus, these are not discussed above because these are test cases not formally submitted for SAMPL, but some discussion is warranted. Both of these submissions were done in a blind manner, just as the rest of the SAMPL, and submission 300 (but not 301) was done prior to the submission deadline. Submission 300 was a control run in which a beginning high school student in the Mobley laboratory predicted binding modes using AutoDock simply by following online tutorials and documentation, with no separate instruction and with minimal background reading on IN and on this particular series. It appears that one major challenge for 300 was the definition of and identification of the binding site region. Very few ligands were placed nearest the correct site, and even of those, none came close to the correct binding modes.

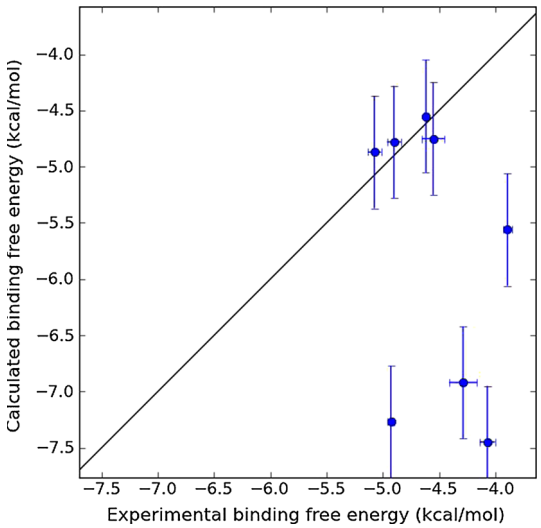


**Fig. 7** Performance of submission 184 in the integrase affinity challenge. While one group of compounds was well predicted, another group was not. 184 was essentially the top submission in the challenge

Primarily, this probably serves to illustrate that some expertise in docking and some knowledge of likely binding sites is still needed for successful pose prediction.

ID 301 provides a more challenging benchmark. This applied a different approach than most participants, and took all six bound ligands out of the 3NF8 reference structure. Each ligand was then shape-overlaid onto the 3NF8 ligands using OpenEye's ROCS, and bumping poses were removed. Each pose was then energy minimized with MMFF, and the remaining pose with the best MMFF energy was then submitted. This actually would have ended up being the top submission by most metrics, and does extremely well. This is partly because this is precisely the type of challenge where a ligand-based approach such as this one ought to do well—where there are structures of related ligands bound in all the binding sites of interest—and partly because the LEDGF site seems to have typically resulted in the best MMFF energy.

We examined median error across different ligands in the set to try and understand whether particular classes of ligand were especially difficult to predict. However, almost every ligand is well predicted by at least some methods. Median errors across all methods do fluctuate substantially from ligand-to-ligand, but we did not immediately observe patterns where particular classes or groups of ligands were particularly difficult to predict. We did observe a slight correlation between increasing molecular weight and median RMSD, but some correlation between RMSD and molecular weight is to be expected regardless. We also find (as did Coleman et al. [8]) a slight trend that more highly charged ligands (charge −2, or zwitterions with charge −2 + 1) may have higher median RMSDs, but the test set is small enough it is hard to be sure this is statistically significant.

## Integrase affinity results

The integrase affinity challenge received 15 submissions from four groups. Statistics are shown in Table 3 and Fig. 6. We used the Kendall W statistic to see whether there was a clear leader and arrived at a value of $W = 0.80 \pm 0.08$, indicating that almost all affinities are better predicted by one submission than any other. This submission was 184 (Fig. 7), which used the SIE scoring function [38, 48] with the FiSH [9] hydration model, but even this suffered from rather poor performance overall. While this submission's RMS error, 1.83 ± 0.41 kcal/mol, and the AUE 1.33 ± 0.44 kcal/mol seem acceptable, the experimental data spans only a 1 kcal/mol range, so the error is larger than the signal. Thus, for ID 184, the Pearson R and Kendall tau are actually negative, indicating incorrect ranking. Interestingly, one group of compounds seems well predicted, while the rest are very poorly predicted. The authors suggest that some of this noise can be reduced by using a common protein structure instead of the cognate crystallographic structures [24].

In this challenge component, most submissions actually used docking to try and predict affinities. And submission IDs 199, 201, and 233–237 actually submitted scores from the DOCK package as "affinity" predictions. Since these scores are not normalized, the hope was that these would provide some correlation with experiment, rather than actually provide reasonable affinity estimates, hence the very large errors for these submissions. One notable exception to the typical docking approach here was submissions 190–191, which used an MM-PB/SA approach.

Submission IDs 012 and 013 were a null model based on the classic work of Kuntz [32], where affinities were predicted based on the number of heavy atoms with a value of 1.5 kcal/mol per heavy atom up to a plateau value, and then were a constant beyond that (ID 012). Because all of these ligands are large enough to have reached the plateau, this resulted in a constant prediction for all ligands, so model 013 removes the plateau. These were provided by Coleman et al. [8]. It is worth noting that a variety of other methods substantially outperform these null models here, despite the limited nature of this test.

Overall, given the very narrow range of experimental binding free energies for these few relatively weak ligands, it is difficult to draw any strong conclusions from this portion of the challenge.

## Conclusions

Overall, the HIV integrase portion of the SAMPL4 challenge proved extremely challenging. The virtual screening component was difficult apparently because the inactive compounds are true inactives and were so similar to active compounds, and indeed were tested precisely because they were thought to bind. Thus, it proved extremely difficult to substantially enrich compounds in this portion of the challenge. Likewise, the binding mode prediction of the challenge was difficult, partly because of the several binding sites participants had to deal with. And the narrow range of relatively weak affinities in the affinity prediction challenge made it challenging to achieve any correlation between calculated and experimental values—though several methods did have reasonably low errors.

However, it was encouraging that some methods were able to significantly enrich actives in the virtual screening portion of the challenge. Here, one method in particular stood out from the pack, and interestingly, it involved substantial manual intervention from a human expert in the screening process. Apparently, human expertise still pays off. To us, this is actually somewhat encouraging, in that it means that there is still more we can teach our binding prediction algorithms.

For binding mode prediction, all methods performed poorly on at least some ligands, but one major source of large errors was placement of ligands into the incorrect binding site (since three binding sites were possible). Interestingly, however, placing ligands into the correct binding site was not a guarantee of success, and some of the top methods actually considered binding to all three sites. This suggests that, at least in some cases, binding site identification may be possible with today's methods. Interestingly, a control model we ran using a ligand-based approach actually performed quite well at this portion of the challenge, suggesting that in the future, participants may want to consider alternate approaches such as this to help their structure-based efforts. A similar (control) ligand-based approach also performed well in the virtual screening test, further supporting this line of thinking. Possibly in future challenges the best approach may involve a combination of methods.

Overall, we believe the integrase component of the SAMPL4 challenge was a valuable test, and we are convinced that blind tests like this are a helpful way to gain insight into how methods may perform in a real-world discovery setting. Expert knowledge does seem to continue to play an important role, but it does not guarantee success, nor does the lack of expert knowledge guarantee failure. Much depends on both the practitioner and the details of the approach.

## Supporting information

We provide Supporting Information in the form of a supporting archive file which contains the majority of the challenge inputs, outputs, and analysis and plots generated. Specifically, it contains the intro PDF file which was provided to participants, and all challenge inputs as provided to participants. Additional files are provided indicating changes which were made (in the form of molecules removed) prior to analysis, and experimental results are provided. We provide all statistics computed, and the full set of plots generated for all submissions in all challenge components. Additionally, for participants who consented, we provide the contents of their submissions, including method descriptions and other metadata.

**Acknowledgments** We acknowledge the financial support of the National Institutes of Health (1R15GM096257-01A1 to DLM and R01 GM073087 and P50 GM103368 to AJO), and computing support from the UCI GreenPlanet cluster, supported in part by NSF Grant CHE-0840513. We are also grateful to OpenEye Scientific Software for support for SAMPL, including for the meeting and for logistical help with the website, and in particular would like to thank Matt Geballe for help with the website and submissions and for helpful discussions, and Paul Hawkins, Greg Warren, and Geoff Skillman for helpful discussions and pointers on analysis. We are also thankful to Tom Peat (CSIRO) and colleagues for the experimental data which made the integrase portion of SAMPL possible, and helped initiate SAMPL4.

## References

1. Abram ME, Hluhanich RM, Goodman DD, Andreatta KN, Margot NA, Ye L, Niedziela-Majka A, Barnes TL, Novikov N, Chen X, Svarovskaia ES, McColl DJ, White KL, Miller MD (2013) Impact of primary Elvitegravir resistance-associated mutations in HIV-1 integrase on drug susceptibility and viral replication fitness. Antimicrob Agents Chemother 57(6): 2654–2663
2. Benson ML, Faver JC, Ucisik MN, Dashti DS, Zheng Z, Merz KM Jr (2012) Prediction of trypsin/molecular fragment binding affinities by free energy decomposition and empirical scores. J Comput Aided Mol Des 26(5):647–659
3. Blow DM (2002) Rearrangement of Cruickshank's formulae for the diffraction-component precision index. Acta Crystallogr Sect D Biol Crystallogr 58(5):792–797
4. Cherepanov P, Ambrosio ALB, Rahman S, Ellenberger T, Engelman A (2005) Structural basis for the recognition between HIV-1 integrase and transcriptional coactivator p75. Proc Natl Acad Sci USA 102(48):17,308–17,313
5. Chodera JD, Mobley DL, Shirts MR, Dixon RW, Branson K, Pande VS (2011) Alchemical free energy methods for drug discovery: progress and challenges. Curr Opin Struct Biol 21(2): 150–160
6. Christ F, Shaw S, Demeulemeester J, Desimmie BA, Marchand A, Butler S, Smets W, Chaltin P, Westby M, Debyser Z, Pickford C (2012) Small-molecule inhibitors of the LEDGF/p75 binding site of integrase block HIV replication and modulate

integrase multimerization. Antimicrob Agents Chemother 56(8): 4365–4374
7. Christ F, Voet A, Marchand A, Nicolet S, Desimmie BA, Marchand D, Bardiot D, Vander Veken NJ, Van Remoortel B, Strelkov SV, De Maeyer M, Chaltin P, Debyser Z (2010) Rational design of small-molecule inhibitors of the LEDGF/p75-integrase interaction and HIV replication. Nat Meth 6(6):442–448
8. Coleman RG, Sterling T, Weiss DR (2014) SAMPL4 & DOCK3.7: lessons for automated docking procedures. J Comput Aided Mol Des. doi:10.1007/s10822-014-9722-6
9. Corbeil CR, Sulea T, Purisima EO (2010) Rapid prediction of solvation free energy. 2. The first-shell hydration (FiSH) continuum model. J Chem Theory Comput 6(5):1622–1637
10. De Clercq E (1999) Perspectives of non-nucleoside reverse transcriptase inhibitors (NNRTIs) in the therapy of HIV-1 infection. Il Farmaco 54(1–2):26–45
11. Dewdney TG, Wang Y, Kovari IA, Reiter SJ, Kovari LC (2013) Reduced HIV-1 integrase flexibility as a mechanism for raltegravir resistance. J Struct Biol 184:245–250
12. Engelman A, Cherepanov P (2012) The structural biology of HIV-1: mechanistic and therapeutic insights. Nat Rev Microbiol 10(4):279–290
13. Ewing TJ, Makino S, Skillman AG, Kuntz ID (2001) DOCK 4.0: search strategies for automated molecular docking of flexible molecule databases. J Comput Aided Mol Des 15(5):411–428
14. Friesner RA, Murphy RB, Repasky MP, Frye LL, Greenwood JR, Halgren TA, Sanschagrin PC, Mainz DT (2006) Extra precision glide: docking and scoring incorporating a model of hydrophobic enclosure for proteinligand complexes. J Med Chem 49(21): 6177–6196
15. Gallicchio E, Deng N, He P, Perryman AL, Santiago DN, Forli S, Olson AJ, Levy RM (2014) Virtual screening of integrase inhibitors by large scale binding free energy calculations. J Comput Aided Mol Des. doi:10.1007/s10822-014-9711-9
16. Gallicchio E, Lapelosa M, Levy RM (2010) The binding energy distribution analysis method (BEDAM) for the estimation of protein-ligand binding affinities. J Chem Theory Comput 6(9): 2961–2977
17. Geretti AM, Armenia D, Ceccherini-Silberstein F (2012) Emerging patterns and implications of HIV-1 integrase inhibitor resistance. Curr Opin Infect Dis 25(6):677–686. doi:10.1097/QCO.0b013e32835a1de7
18. Greenwald J, Le V, Butler SL, Bushman FD, Choe S (1999) The mobility of an HIV-1 integrase active site loop is correlated with catalytic activity. Biochemistry 38(28):8892–8898
19. Hare S, Maertens GN, Cherepanov P (2012) 3[prime]-Processing and strand transfer catalysed by retroviral integrase in crystallo. EMBO J 31(13):3020–3028
20. Hare S, Smith SJ, Métifiot M, Jaxa-Chamiec A, Pommier Y, Hughes SH, Cherepanov P (2011) Structural and functional analyses of the second-generation integrase strand transfer inhibitor dolutegravir (S/GSK1349572). Mol Pharmacol 80(4): 565–572
21. Hare S, Vos AM, Clayton RF, Thuring JW, Cummings MD, Cherepanov P (2010) Molecular mechanisms of retroviral integrase inhibition and the evolution of viral resistance. Proc Natl Acad Sci 107(46):20,057–20,062
22. Hawkins PCD, Nicholls A (2012) Conformer generation with OMEGA: learning from the data set and the analysis of failures. J Chem Inf Model 52(11):2919–2936
23. Hawkins PCD, Skillman AG, Warren GL, Ellingson BA, Stahl MT (2010) Conformer generation with OMEGA: algorithm and validation using high quality structures from the Protein Databank and Cambridge Structural Database. J Chem Inf Model 50(4):572–584
24. Hogues H, Sulea T, Purisima EO (2014) Exuastive docking and solvated interaction energy scoring: lessons learned from the SAMPL4 challenge. J Comput Aided Mol Des. doi:10.1007/s10822-014-9715-5
25. Japrung D, Leartsakulpanich U, Chusacultanachai S, Yuthavong Y (2007) Conflicting requirements of Plasmodium falciparum dihydrofolate reductase mutations conferring resistance to pyrimethamine-WR99210 combination. Antimicrob Agents Chemother 51(12):4356–4360
26. Jurado KA, Wang H, Slaughter A, Feng L, Kessl JJ, Koh Y, Wang W, Ballandras-Colas A, Patel PA, Fuchs JR, Kvaratskhelia M, Engelman A (2013) Allosteric integrase inhibitor potency is determined through the inhibition of HIV-1 particle maturation. Proc Natl Acad Sci 110(21):8690–8695
27. Kessl JJ, Jena N, Koh Y, Taskent-Sezgin H, Slaughter A, Feng L, de Silva S, Wu L, Le Grice SFJ, Engelman A, Fuchs JR, Kvaratskhelia M (2012) Multimode, cooperative mechanism of action of allosteric HIV-1 integrase inhibitors. J Biol Chem 287(20): 16,801–16,811
28. Krishnan L, Engelman A (2012) Retroviral integrase proteins and HIV-1 DNA integration. J Biol Chem 287(49):40,858–40,866
29. Kuhn B, Kollman PA (2000) Binding of a diverse set of ligands to avidin and streptavidin: an accurate quantitative prediction of their relative affinities by a combination of molecular mechanics and continuum solvent models. J Med Chem 43(20):3786–3791
30. Kulp JL, Blumenthal SN, Wang Q, Bryan RL, Guarnieri F (2012) A fragment-based approach to the SAMPL3 challenge. J Comput Aided Mol Des 26(5):583–594
31. Kumar A, Zhang KYJ (2012) Computational fragment-based screening using RosettaLigand: the SAMPL3 challenge. J Comput Aided Mol Des 26(5):603–616
32. Kuntz ID, Chen K, Sharp KA, Kollman PA (1999) The maximal affinity of ligands. Proc Natl Acad Sci 96(18):9997–10,002
33. Lindorff-Larsen K, Piana S, Palmo K, Maragakis P, Klepeis JL, Dror RO, Shaw DE (2010) Improved side-chain torsion potentials for the Amber ff99SB protein force field. Proteins pp NA–NA 78(8):1950–1958
34. Maertens GN, Hare S, Cherepanov P (2010) The mechanism of retroviral integration from X-ray structures of its key intermediates. Nature 468(7321):326–329
35. MarvinSketch version 5.8.2 (2013)ChemAxon. http://www.chemaxon.com/products/marvin/marvinsketch/
36. Métifiot M, Maddali K, Johnson BC, Hare S, Smith SJ, Zhao XZ, Marchand C, Burke TR, Hughes SH, Cherepanov P, Pommier Y (2013) Activities, crystal structures, and molecular dynamics of dihydro-1H-isoindole derivatives, inhibitors of HIV-1 integrase. ACS Chem Biol 8(1):209–217
37. Mobley DL, Wymer KL, Lim NM (2014) Blind prediction of solvation free energies from the SAMPL4 challenge. J Comput Aided Mol Des
38. Naïm M, Bhat S, Rankin KN, Dennis S, Chowdhury SF, Siddiqi I, Drabik P, Sulea T, Bayly CI, Jakalian A (2007) Solvated interaction energy (SIE) for scoring protein-ligand binding affinities. 1. Exploring the parameter space. J Chem Inf Model 47(1):122–133
39. Newman J, Dolezal O, Fazio V, Caradoc-Davies T, Peat TS (2012) The DINGO dataset: a comprehensive set of data for the SAMPL challenge. J Comput Aided Mol Des 26(5):497–503
40. Nicholls A, Mobley DL, Guthrie JP, Chodera JD, Bayly CI, Cooper MD, Pande VS (2008) Predicting small-molecule solvation free energies: an informal blind test for computational chemistry. J Med Chem 51(4):769–779
41. OpenEye Python Toolkits. http://www.eyesopen.com (2013)
42. Peat TS, Dolezal O, Newman J, Mobley DL, Deadman JJ (2014) Interrogating HIV integrase for compounds that bind—a

SAMPL4 challenge. J Comput Aided Mol Des. doi:10.1007/s10822-014-9721-7
43. Peat TS, Warren G (2013) Personal Communication. E-mail exchange
44. Perryman AL, Forli S, Morris GM, Burt C, Cheng Y, Palmer MJ, Whitby K, McCammon JA, Phillips C, Olson AJ (2010) A dynamic model of HIV integrase inhibition and drug resistance. J Mol Biol 397(2):600–615
45. Quashie PK, Mesplède T, Han YS, Veres T, Osman N, Hassounah S, Sloan R, Xu HT, Wainberg MA (2013) Biochemical analysis of the role of G118R-linked dolutegravir drug resistance substitutions in HIV-1 integrase. Antimicrob Agents Chemother 57(12):6223–6235
46. Quashie PK, Mesplède T, Wainberg MA (2013) Evolution of HIV integrase resistance mutations. Curr Opin Infect Dis 26(1):43–49. doi:10.1097/QCO.0b013e32835ba81c
47. Skillman AG, Warren GL, Nicholls A (2008) SAMPL at first glance: So much data, so little time…. http://www.eyesopen.com/2008_cup_presentations/CUP9_Skillman.pdf
48. Sulea T, Cui Q, Purisima EO (2011) Solvated interaction energy (SIE) for scoring protein–ligand binding affinities. 2. Benchmark in the CSAR-2010 scoring exercise. J Chem Inf Model 51(9):2066–2081
49. Sulea T, Hogues H, Purisima EO (2012) Exhaustive search and solvated interaction energy (SIE) for virtual screening and affinity prediction. J Comput Aided Mol Des 26(5):617–633
50. Surpateanu G, Iorga BI (2012) Evaluation of docking performance in a blinded virtual screening of fragment-like trypsin inhibitors. J Comput Aided Mol Des 26(5):595–601
51. Trott O, Olson AJ (2010) AutoDock Vina: improving the speed and accuracy of docking with a new scoring function, efficient optimization, and multithreading. J Comput Chem 31(2):455–461
52. Truchon J, Bayly CI (2007) Evaluating virtual screening methods: good and bad metrics for the "early recognition" problem. J Chem Inf Model 47(2):488–508
53. Tsiang M, Jones GS, Niedziela-Majka A, Kan E, Lansdon EB, Huang W, Hung M, Samuel D, Novikov N, Xu Y, Mitchell M, Guo H, Babaoglu K, Liu X, Geleziunas R, Sakowicz R (2012) New class of HIV-1 integrase (IN) inhibitors with a dual mode of action. J Biol Chem 287(25):21,189–21,203
54. Voet ARD, Kumar A, Berenger F, Zhang KYJ (2014) Combining in cerebra and in silico approaches for virtual screening and pose prediction in SAMPL4. J Comput Aided Mol Des. doi:10.1007/s10822-013-9702-2
55. Wainberg MA, Mesplède T, Quashie PK (2012) The development of novel HIV integrase inhibitors and the problem of drug resistance. Curr Opin Virol 2(5):656–662
56. Wang J, Wolf R, Caldwell J, Kollman P, Case D (2004) Development and testing of a general amber force field. J Comput Chem 25(9):1157–1174
57. Wang R, Liu L, Lai L, Tang Y (1998) SCORE: a new empirical method for estimating the binding affinity of a protein-ligand complex. J Mol Model 4(12):379–394
58. Zhang J, Adrian FJ, Jahnke W, Cowan-Jacob SW, Li AG, Iacob RE, Sim T, Powers J, Dierks C, Sun F, Guo GR, Ding Q, Okram B, Choi Y, Wojciechowski A, Deng X, Liu G, Fendrich G, Strauss A, Vajpai N, Grzesiek S, Tuntland T, Liu Y, Bursulaya B, Azam M, Manley PW, Engen JR, Daley GQ, Warmuth M, Gray NS (2010) Targeting Bcr-Abl by combining allosteric with ATP-binding-site inhibitors. Nature 463(7280):501–506